INTERNATIONAL JOURNAL OF INNOVATIVE RESEARCH & DEVELOPMENT

ISSN 2278 – 0211 (Online)

Evaluation of the Downwind Dispersion of Gaseous Emissions from Cement Milling and Grinding Facilities in Athi River, Machakos County, Kenya

Jermaine O. Omulami
Student, Department of Chemistry, University of Nairobi, Nairobi, Kenya
Patrick K. Tum
Lecturer, Department of Chemistry, University of Nairobi, Nairobi, Kenya
Rachael E. N. Njogu
Lecturer, Department of Chemistry, University of Nairobi, Nairobi, Kenya
Dickson M. Andala
Lecturer, Department of Chemistry, Multimedia University of Kenya, Nairobi Kenya
George O. Achieng
Student, Department of Chemistry, Maseno University, Maseno, Kenya

Abstract:
Cement manufacturing results in the release of gaseous emissions, which cause air pollution. Air pollution affects human health. In this study, two cement grinding and milling facilities in Athi River, Machakos County, in Kenya, were selected to determine the downwind dispersion of flue gases (CO, CO_2, SO_2 and NO_x) emitted into the environment using AERMOD software. Cement Factory 1 (CF1) contained one sampling point (Stack 1) and Cement Factory 2 (CF2) contained two points (Stacks 2a and 2b). The sampling procedures were based on the Environmental Protection Agency (EPA) standard methods. Unlike CO_2, the modelling results showed that the maximum peak concentrations of CO, SO_2 and NO_x were below the permissible limits under the EMCA 2014 and WHO Air Quality Guidelines 2021. The 8-hour and 1-hour mean maximum concentration was 8.809±1.570 mg/m^3 and 32.715±4.362 mg/m^3, respectively. Both stack 2a and 2b recorded negligible concentrations of CO, SO_2 and NO_x.

Keywords: *Air pollution, air dispersion modelling, cement manufacturing, gaseous emissions*

1. Introduction

In recent years, air quality degradation has slowly developed to be an important issue in the world (Sen et al., 2023). With Kenya striving to attain Vision 2030 aimed at transforming itself into an industrialized, middle-income country, degradation of air quality is likely to increase if not properly monitored. Industrial development involves an increase in the utilization of fossil fuels which in turn increases atmospheric emissions (Jittra et al., 2015). Common air pollutants include volatile organic compounds (VOCs) such as benzene and toluene, carbon monoxide (CO), nitrogen oxides (NOx), carbon dioxide (CO2), particulate matter (PM10 and PM2.5), sulphur dioxide (SO2), ozone (O3) and heavy metals such as arsenic, lead and mercury among others (Manisalidis et al., 2020).

In Kenya, the cement manufacturing industry is growing at a very fast rate due to the continuous increase in demand. The sector provides a means of better housing and creates employment opportunities, facilitating economic growth (Devi et al., 2017; Eshikumo & Odock, 2017). Most of the cement industries in Kenya are located in Athi River in Machakos County and Mombasa. This is attributed to the availability of raw materials.

Cement manufacturing involves burning limestone-based raw materials, which release carbon dioxide gas as a by-product (Ali et al., 2011). Apart from carbon dioxide, some common emissions released by the cement industry include carbon monoxide, nitrogen dioxide, sulphur dioxide and particulate matter (Ali et al., 2011). Air pollution poses adverse health effects to the general population. Atmospheric pollution has been linked to lung cancer, chronic obstructive pulmonary diseases, stroke, acute respiratory infections and heart diseases, which increase mortality rates (Ibrahim et al., 2012; WHO, 2019). Air pollution accounts for approximately 19000 premature deaths in Kenya, as claimed by The State of the Global Air 2019 report (deSouza, 2020). Poor health negatively affects the individual's productivity and adversely affects the country's economy (Jittra et al., 2015). Air pollution prevention and control strategies are, therefore, essential aspects to consider in attaining Vision 2030.

Atmospheric dispersion modelling predicts the downwind transportation and dispersion of specific pollutants and hence the ambient concentration of the atmospheric emissions at a given receptor (Schnelle & Brown, 2001). The

extent of downwind transportation of air pollutants is determined by the topography and meteorological conditions of the area (Turner, 1994), the height of the emitting stack and the existing nearby buildings and structures (Schnelle & Brown, 2001). By combing these factors, modelling can be used to determine the pollutants concentrations in various regions and determine the affected recipients (Schnelle & Brown, 2001). For this reason, modelling can not only be used to determine the extent of air pollution by existing industries but can also be used to predict the effects of future industrial projects (Barratt, 2001). A common example of an atmospheric dispersion model is the American Meteorological Society/Environmental Protection Regulatory Model (AERMOD).

In Kenya, AERMOD has been used to predict future concentrations of hydrogen sulphide (H2S) from a proposed Geothermal Plant in Menengai (Ndetei, 2010; Nyairo & Onyancha, 2018). The research concluded that the hydrogen sulphide concentrations from the power plant would be below the World Health Organisation (WHO) guidelines of 150 µgm-3. Several research studies have been able to link various point sources to the deterioration of human health. For instance, Kiano (2018) studied the health effects of industrial pollution of the pulp and paper industry in Webuye on the residents living in the area. The study reported the mean emission rate of particulate matter in Webuye town was 102.17 µgm-3. In addition, the study showed that there was a significant variance in respiratory tract infections among the residents between the periods when emissions were being released between 2007 and 2009 and the post-emission period, from 2014 to 2015. In addition, seven out of ten respondents had a persistent cough during the emission period (Kiano, 2018).

2. Materials and Methods

2.1. Sampling Area

Stack emission analysis was carried out from two selected cement factories (Cement Factory 1, CF1 and Cement Factory 2, CF2) in Athi River Machakos County in Kenya. Athi River is a town on the outskirts of Nairobi in Machakos County located in the UTM coordinates (37S 275033.42mE 9838954.72mS). CF1 contained one stationary source (Stack 1) and CF2 contained two (Stack 2a and 2b) from which sampling was done. Both cement factories receive readymade clinkers. The clicker received at CF1 undergoes milling and drying using a diesel-powered vertical roller mill (VRM) dryer. CF2 is a dry grinding facility that grinds and mills the readymade clinker with 5% gypsum using a ball mill.

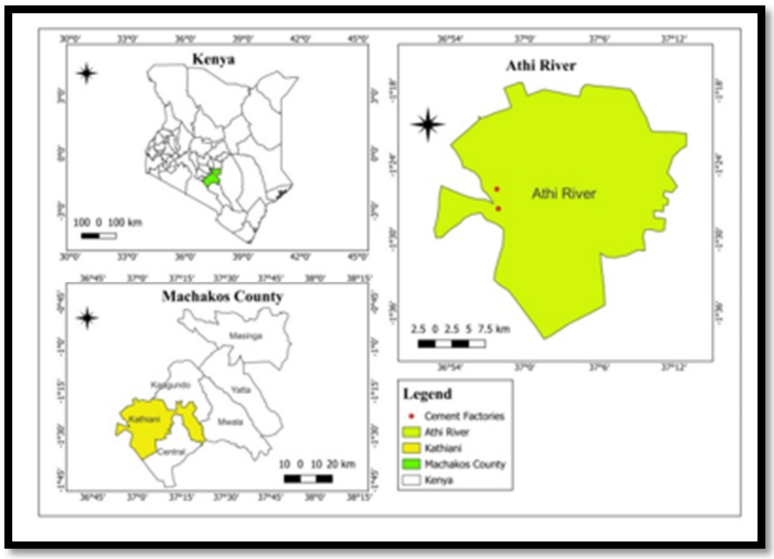

Figure 1: Study Area

2.2. Source Data

Source data included source location and release parameters such as emission rate, stack gas exit velocity and temperature and stack gas flow rate, as shown in tables 1, 2, 3 & 4. The stack emission rate was calculated from the stack emission concentration of the gases determined using an Emission analyser E6000-5SC. The concentration of gaseous emissions was determined by inserting the probe into the stack to draw the gaseous mixture from the stack using an inbuilt pump. After about twenty minutes, the gas concentrations were recorded. The sampling was done in triplicate. Stack emission gas flow rate, exit velocity and exit temperature were determined using an Isokinetic Source Sampler-XC-572-VStack Emission Concentration.

	Stack 1	Stack 2a	Stack 2b
Location	(37S, 273381.45 mE, 9838633.10 mS)	(37S, 273329.86 mE, 9841673.43 mS)	(37S, 273284.21 mE, 9841628.73 mS)
Stack Height (m)	35	39	45
Stack Diameter (m)	1.8	1.5	1.5
Elevation (m)	1539	1512	1514

Table 1: Source Location Data

	Sample 1	Sample 2	Sample 3	Average
Gas Exit Temp (^{0}C)	12.25	12.167	16.583	13.6667
Gas Exit Velocity (m/s)	3.9719	4.0566	4.1233	4.0506
Emission rates (g/s)				
Sulphur dioxide	0.0646	0.0569	0.0432	0.0549
Nitrogen oxides	0.1912	0.1931	0.2321	0.2055
Carbon dioxide	276.99	213.93	252.43	247.78
Carbon monoxide	0.0077	0.0084	0.0065	0.0075

Table 2: Emission Source Data CF1 Stack 1

	Sample 1	Sample 2	Sample 3	Average
Gas Exit Temp (^{0}C)	15.792	13.333	13.917	14.3473
Gas Exit Velocity (m/s)	6.4721	6.4405	6.4934	6.4687
	Emission rates (g/s)			
Carbon dioxide	3.6331	1.8102	1.7873	2.41

Table 3: Emission Source Data CF2 Stack 2a

	Sample 1	Sample 2	Sample 3	Average
Gas Exit Temp (^{0}C)	14.508	13.5	13.167	13.725
Gas Exit Velocity (m/s)	7.4236	7.1406	6.4634	7.0092
	Emission rates (g/s)			
Carbon dioxide	4.1251	1.9881	1.7885	2.63

Table 4: Emission Source Data CF2 Stack 2b

2.3. Meteorological Data

- *Hourly Surface Data:* The hourly surface data including the measurement hour, day, month and year, relative humidity, temperature, opaque sky cover, wind speed and direction, cloud cover and surface pressure for the period dated between 1st January 2018 and 31st December 2020 was obtained from National Centre for Environmental Information (NCEI) formerly National Climatic Data Centre (NCDC) as reported by Jomo Kenyatta International Airport (JKIA) weather station no. 637400-99999.
- *Upper Air Sounding Data:* Upper air sounding data containing the measurement height and its temperature and pressure were obtained from National Oceanic and Atmospheric Administration Earth System Research Laboratories (NOAA/ESRL) database as reported by the Dagoretti weather meteorological station no. 637410-99999

2.4. Land Use Data

The land use cover at the hourly surface meteorological site was classified according to the National Land Cover Database (NLCD-1992). The area was classified into open water (11), low (21) and high-intensity residential areas (22), commercial/industrial/ transportation (23), shrubland (51) and urban/recreational grasses (85)

2.5. Terrain and Building Data

Terrain data was obtained from the USGS as STRM 1-Arc second global digital elevation data. Buildings surrounding the stack likely to cause downwash were selected based on the structure influence zone.

2.6. Receptor Data

The simulation was done at a square distance of 10km by 10km centred at the point source. The concentrations were simulated at a flagpole height of 1.50m, the approximate breathable height. Uniform Cartesian Grid with a grid resolution of 50m by 50m within the first 5 km by 5km square distance and 200m by 200m up to the 10km by 10km square distance centred at the point source.

2.7. Output

The concentration of each receptor was represented as a contour plot file for the 1st highest 24-hour period for SO_2 and NO_x and the 1st highest 8-hour period for carbon dioxide and carbon monoxide. The mean maximum concentration, as predicted by the model, was recorded. The concentrations observed at the selected discrete receptor

boundaries were also recorded. The above concentrations were compared with the ambient tolerance limits stipulated under EMCA, 2014 (NEMA, 2014) and WHO Air Quality Guidelines, 2021 (WHO, 2021).

3. Results and Discussions

3.1. Wind Speed and Direction

Figure 2 shows the wind-rose showing the speed and direction of the wind.

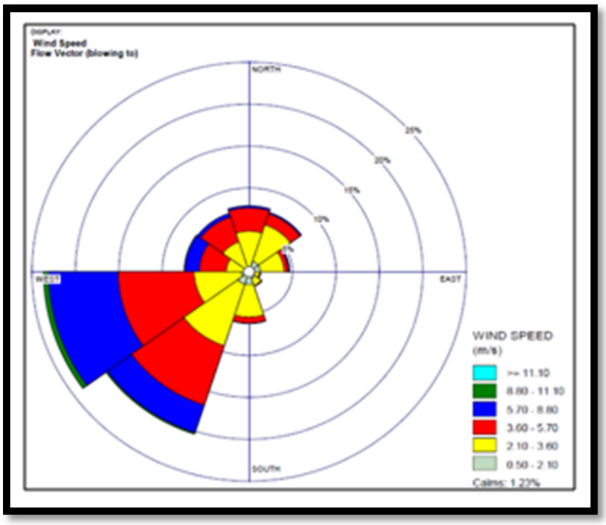

Figure 2: Wind-Rose

Figure 2 shows the wind blew approximately 23% of the time towards the west at a speed of 0.50-2.10 m/s about 0.5% of the time, 2.10-3.60 m/s about 4.5% of the time, 3.60-5.70 m/s about 10% of the time, 5.70-8.80 m/s about 12% of the time and 8.80-11.10 m/s about 1% of the time. The wind was also predominant towards the south-west, blowing approximately 20% of the time at a speed of 0.50-2.10 m/s about 1% of the time, 2.10-3.60 m/s about 8% of the time, 3.60-5.70 m/s about 9% of the time, 5.70-8.80 m/s about 3% of the time and 8.80-11.10 m/s about 0.5% of the time. The wind blew approximately 7.5% of the time towards other directions apart from the south-east, where it was less than 5% of the time of assessment. During the data collection period, the average wind speed was 3.46 m/s and the percentage of calm winds was 1.23%.

3.2. Peak Maximum Concentration

The modelling results from CF1 and CF2 were expressed as the 1st highest maximum concentration at a flagpole height of 1.5m, shown in tables 5 and 6. The point of maximum concentration occurred at 49.99m heading 89.88o from CF1 and 117.72m heading 26.43o from CF2. The deposition occurred just a short distance from the stationary points of the cement factory. The deposition over the short distance was likely due to the short stacks compared to the surrounding buildings (Turner, 1994). To reduce the ground-level concentration, it is advisable to install a stack with a height of at least 2.5 times that of the tallest (Schnelle & Brown, 2001). According to good engineering practices the recommended stack height for Stacks 1, 2a and 2b are 74.02 m, 116.86 m and 92.08 m, respectively, from their existing stack heights of 35 m, 39 m and 45 m. Downwind dispersion of carbon monoxide, sulphur dioxide and nitrogen oxides from CF2 was not done because the stack concentration was below the detection limit, hence negligible emission rate.

		Sample 1	Sample 2	Sample 3	Average	WHO	NEMA
CO_2	8-hr	10.619	7.811	7.998	8.809±1.57	NP	2
(mg/m^3)	1-hr	36.907	28.201	33.038	32.715±4.362	NP	4
CO	8-hr	0.00029	0.00031	0.00021	0.00027±0.00005	NP	2
(mg/m^3)	1-hr	0.00102	0.00102	0.00085	0.00096±0.0001	4	4
SO_2	Annual	0.231	0.203	0.153	0.196±0.0395	NP	60
($\mu g/m^3$)	24-hr	1.148	0.95	0.709	0.936±0.220	40	80
NO_x	Annual	0.685	0.688	0.822	0.731±0.0782	10	60
($\mu g/m^3$)	24-hr	3.4	3.225	3.808	3.478±0.299	25	80
*NP – Not provided							

Table 5: Maximum Ambient Concentration from CF1

		Sample 1	Sample 2	Sample 3	Average	WHO	NEMA
CO_2 (mg/m^3)	8-hr	0.571	0.59	0.579	0.58±0.0095	NP	2
	1-hr	4.727	2.367	2.334	3.143±1.372	NP	4
*NP – Not provided							

Table 6: Maximum Ambient Concentration from CF2

3.3. Carbon Dioxide

The modelling results for carbon dioxide from CF1 and CF2 are shown in tables 5 & 6 and figures 3, 4 & 5. Figures 4 & 5 show the contour representation of the modelling results with the highest maximum ambient concentration among the sample runs done.

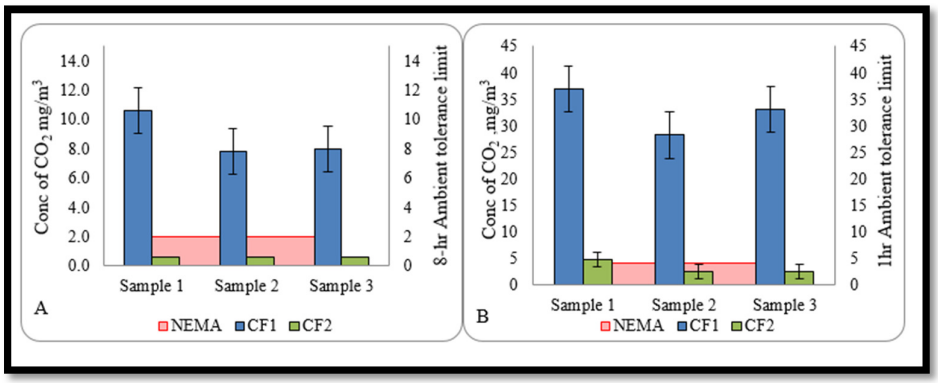

Figure 3: A Graph of the (A) 8-Hour and (B) 1-Hour Maximum Concentration of Carbon Dioxide

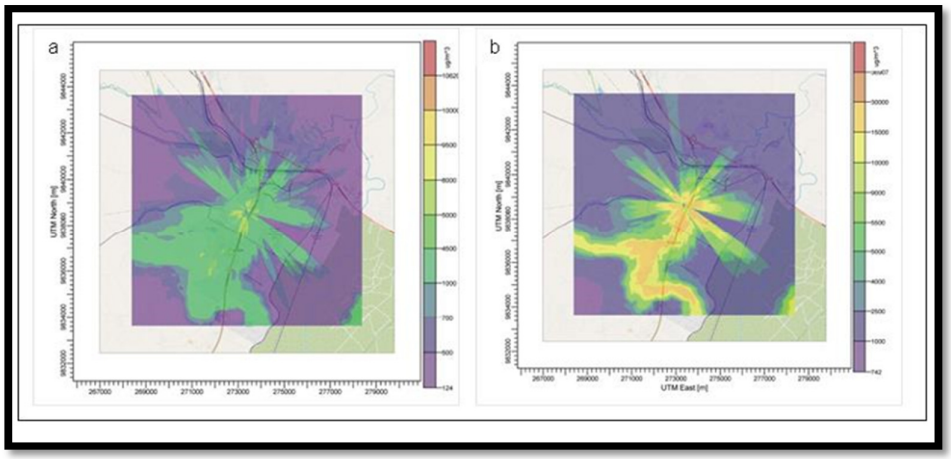

Figure 4: (A) 8-Hour and (B) 1-Hour Ambient Concentration of Carbon Dioxide from CF1

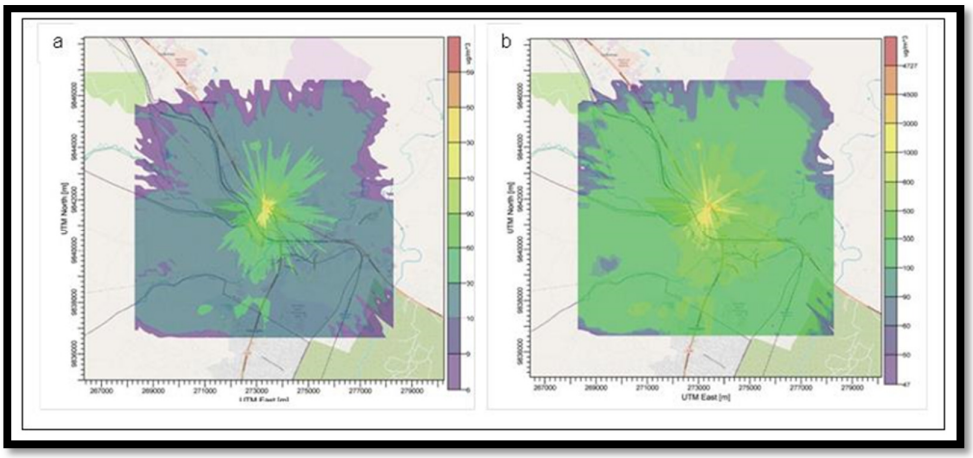

Figure 5: (A) 8-Hour and (B) 1-Hour Ambient Concentration of Carbon Dioxide from CF2

The average 8-hour average maximum concentration of carbon dioxide for CF1 and CF2 were 8.809±1.57 mg/m3 and 0.58±0.0095 mg/m3 and the 1-hour average maximum concentrations were 32.715±4.362 mg/m3 and 3.143±1.372

mg/m3 respectively. Unlike CF2, the average maximum concentrations of CF1 exceeded the ambient tolerance limit of 2 mg/m3 and 4 mg/m3, respectively, as stipulated under EMCA 2014. The high average maximum concentration from CF1 was mainly due to the higher emission rates from Stack 1 compared to Stacks 2a and 2b from CF2. The higher the emission rate, the higher the impact (Westbrook, 1999). The high emission rate is mainly attributed to the burning of diesel for the production of energy used for drying. Diesel readily burns in the air to produce carbon dioxide and water (Chmielewski, 1999).

A higher 8-hour and 1-hour ambient concentration of the pollutants from the emission point is observed around the emission point and towards the South-West direction from the emission point in CF1. The concentration of carbon dioxide from CF2 is, however, evenly distributed within the receptors.

3.4. Carbon Monoxide

The modelling results for carbon monoxide from CF1 are shown in tables 5 & 6 and figures 6 & 7. Figures 6 & 7 show the contour representation of the modelling results with the highest maximum ambient concentration among the sample runs done.

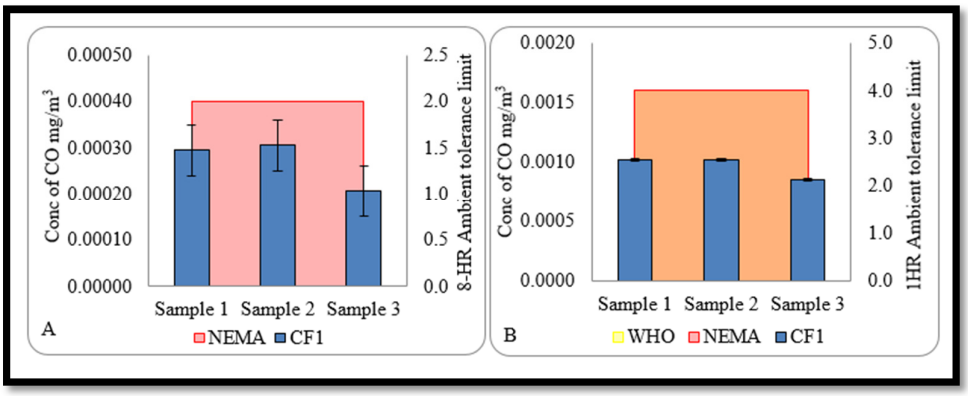

Figure 6: A Graph of the (A) 8-Hour and (B) 1-Hour Maximum Concentration of Carbon Monoxide

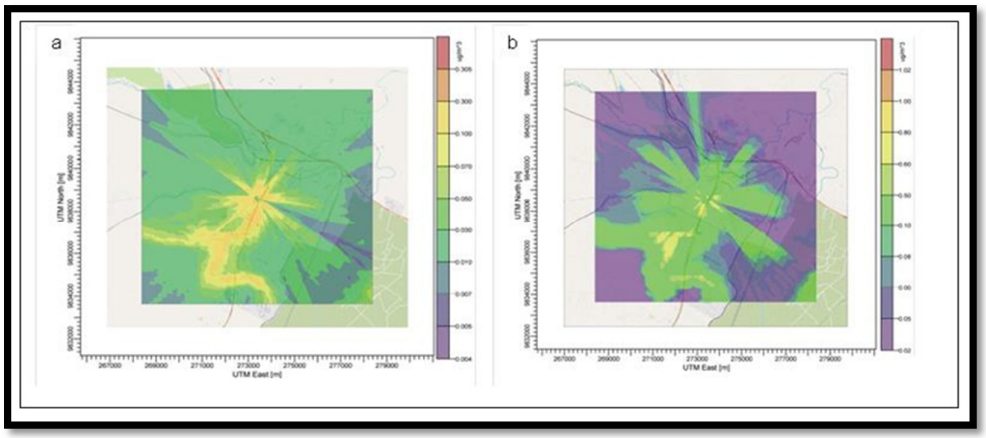

Figure 7: (A) 8-Hour and (B) 1-Hour Ambient Concentration of Carbon Monoxide from CF1

The 8-hour and 1-hour average maximum ambient concentrations of carbon monoxide for CF1 were 0.00027±0.00005 mg/m3 and 0.00096±0.0001 mg/m3, respectively. The maximum ambient concentration of carbon monoxide from CF1 was below the ambient tolerance limit of 2 mg/m3 and 4 mg/m3, respectively, stipulated under EMCA 2014 and the WHO Global Air Quality Guidelines, 2021. The presence of carbon monoxide from CF1 indicates inefficiencies in the combustion process or poor mixing of air with diesel (Manahan, 2017; Rahman et al., 2018).

The higher 8-hour and 1-hour ambient concentration of the pollutants from the emission point in CF1 is observed around the emission point and towards the south-west direction from the emission point.

3.5. Sulphur Dioxide

The modelling results for sulphur dioxide from CF1 are shown in tables 5 & 6 and figures 8 & 9. Figures 8 & 9 show the contour representation of the modelling results with the highest maximum ambient concentration among the sample runs done.

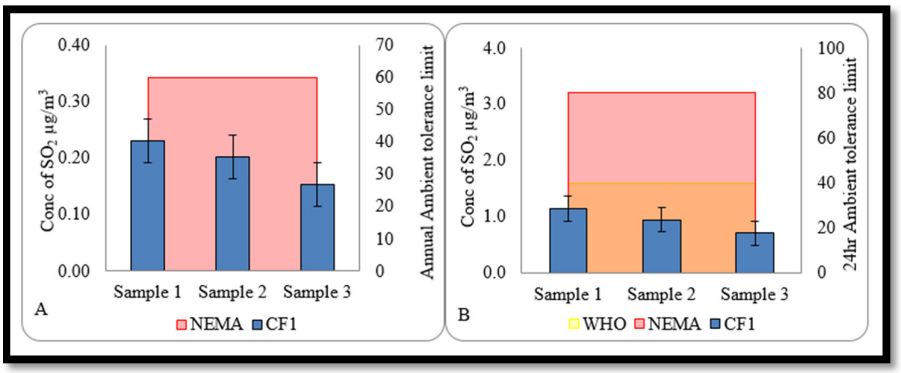

Figure 8: A Graph of the (A) Annual and (B) 24-Hour Ambient Maximum Concentration of Sulphur Dioxide

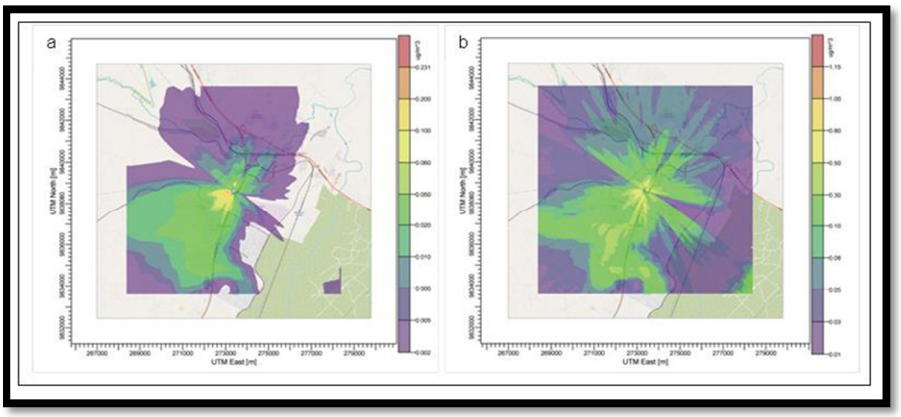

Figure 9: (A) Annual and (B) 24-Hour Ambient Concentration of Sulphur Dioxide from CF1

The annual and 24-hour average maximum ambient concentration of sulphur dioxide for CF1 was 0.196±0.0395 µg/m3 and 0.936±0.220 µg/m3, respectively. The annual and the 24-hour ambient concentration of sulphur dioxide from CF1 was below the ambient tolerance limit of 60 µg/m3 and 80 µg/m3, respectively, stipulated under EMCA 2014 and 40 µg/m3-24-hour ambient tolerance limit under the WHO Global Air Quality Guidelines, 2021. The presence of sulphur dioxide is an indication of traces of sulphur-containing compounds in the diesel used (Rahman et al., 2018).

A higher annual and 24-hour ambient concentration of the pollutants from the emission point is observed around the emission point and towards the South-West direction from the emission point.

3.6. Nitrogen Oxide

The modelling results for sulphur dioxide from CF1 are shown in tables 5 & 6 and figures 10 & 11. Figures 10 & 11 show the contour representation of the modelling results with the highest maximum ambient concentration among the sample runs done.

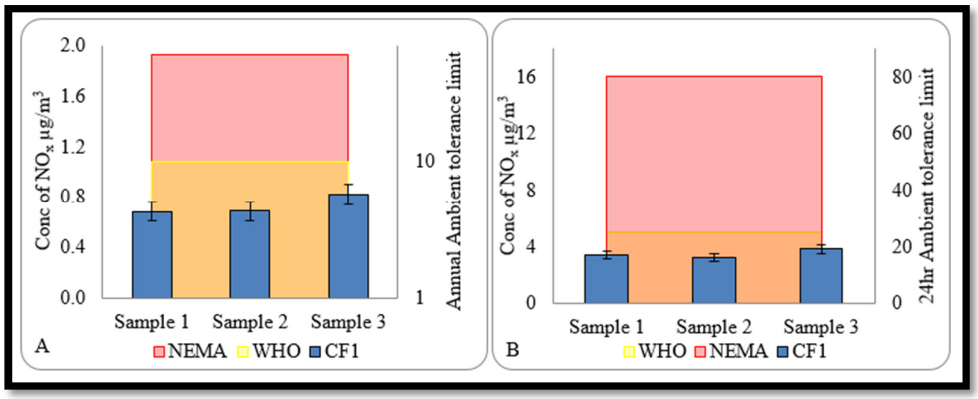

Figure 10: (A) Annual and (B) 24-Hour Maximum Ambient Concentration of Nitrogen Oxides

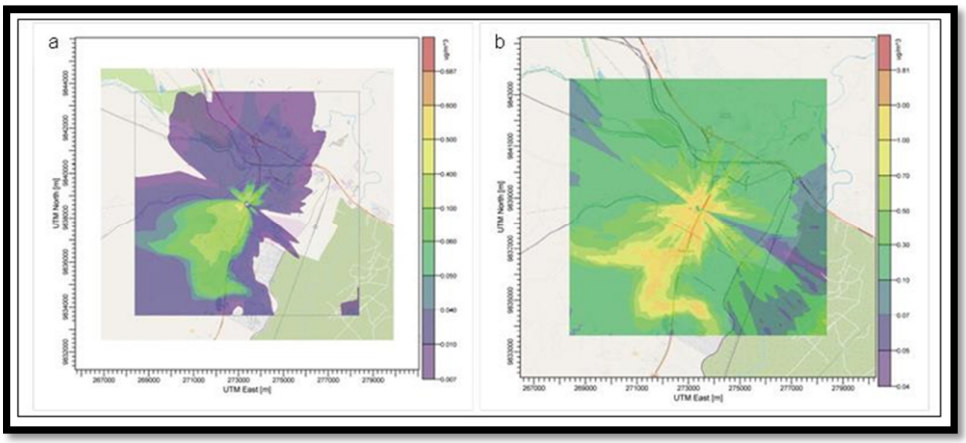

Figure 11: (A) Annual and (B) 24-Hour Ambient Concentration of Nitrogen Oxides from CF1

The annual and 24-hour average maximum concentration of nitrogen oxides for CF1 was 0.731±0.0782 µg/m3 and 3.478±0.299 µg/m3, respectively. The annual and the 24-hour ambient concentration of nitrogen oxides from CF1 was below the ambient tolerance limit of 60 µg/m3 and 80 µg/m3 stipulated under EMCA 2014 and 10 µg/m3 and 25 µg/m3 stipulated under the WHO Global Air Quality Guidelines, 2021 respectively. Nitrogen oxides within the stack mainly form when oxygen combines with nitrogen at elevated temperatures (Ali et al., 2011; Rahman et al., 2018).

A higher annual and 24-hour ambient concentration of the pollutants from the emission point is observed around the emission point and towards the South-West direction from the emission point.

4. Conclusions

Atmospheric dispersion modelling using AERMOD software was carried out to establish the downwind dispersion of gaseous emissions from two selected cement factories. High ambient concentration of the pollutants was observed around the emission points. The maximum concentrations of the pollutants occurred at 49.99 m heading 89.88o for CF1 and 117.72 m heading 26.43o for CF2. The high ambient air concentration around the emission sources was mainly attributed to the low stack height compared to the surrounding buildings. Apart from the surrounding buildings, meteorological conditions affect the transportation of pollutants. The 8-hour and 1-hour maximum ambient concentration of carbon dioxide contributed by CF1 (8.809±1.57 mg/m3 and 32.715±4.362 mg/m3) exceeded the ambient tolerance limit stipulated under EMCA, 2014 and WHO global air quality guidelines, 2021. The high average maximum concentration from CF1 was mainly due to the higher emission rates from Stack 1 compared to Stacks 2a and 2b from CF2. The higher the emission rate, the higher the impact. The high emission rate is mainly attributed to the burning of diesel for the production of energy used for drying. The results and observations made during this study clearly show that the concentrations of emissions from a source determine the ambient concentration of pollutants in the surrounding areas. The higher the emission rate, the higher the impact. It is, therefore, important to ensure that the concentrations of gaseous emissions released from a source are as low as possible. This can be achieved by introducing emission control technologies, flue gas recirculation and using green technology and alternative fuel.

5. Acknowledgement

We thank CSI International Limited for their assistance in sampling. Sampling was carried out by Mr. Omulami and Dr. Oindo. This work was done under the supervision of Dr. Tum, Dr. Rachael and Prof. Andala.

6. References

i. Ali, M. B., Saidur, R., & Hossain, M. S. (2011). A review on emission analysis in cement industries. *Renewable and Sustainable Energy Reviews, 15*(5), 2252–2261. https://doi.org/10.1016/J.RSER.2011.02.014
ii. Barratt, R. (2001). *Atmospheric dispersion modelling: An introduction to practical applications*. Earthscan Ltd.
iii. Chmielewski, A. G. (1999). Environmental effects of fossil fuel combustion. *Interactions: Energy/Environment*, 56–74. https://www.eolss.net/sample-chapters/c09/e4-23-02.pdf
iv. deSouza, P. (2020). Air pollution in Kenya: A review. *Air Quality, Atmosphere & Health, 13*(12), 1487–1495. https://doi.org/10.1007/S11869-020-00902-X
v. Devi, K. S., Lakshmi, V. V., & Alakanandana, A. (2017). Impacts of cement industry on environment: An overview. *Asia Pacific Journal of Research, 1*(57), 2347–4793. www.apjor.com
vi. Eshikumo, S. M., & Odock, S. O. (2017). Green Manufacturing and Operational Performance of a Firm: Case of Cement Manufacturing in Kenya. *International Journal of Business and Social Science, 8*(4), 106–120. www.ijbssnet.com
vii. Ibrahim, H. G., Okasha, A. Y., Elatrash, M. S., & Al-Meshragi, M. A. (2012). Emissions of SO2, NOx, and PMs from Cement Plant in Vicinity of Khoms City in Northwestern Libya. *Journal of Environmental Science and Engineering, 1*, 620–628. https://portal.arid.my/Publications/6a378110-3cdd-43.pdf

viii. Jittra, N., Pinthong, N., & Thepanondh, S. (2015). Performance Evaluation of AERMOD and CALPUFF Air Dispersion Models in Industrial Complex Area. *Aerosol and Air Quality Research, 8*, 87–95. https://doi.org/10.4137/ASWR.S32781

ix. Kiano, E. K. (2018). Economic analysis of health effects of industrial air pollution in Kenya: A case of Webuye and its environs. Retrieved from: http://41.89.164.27:8080/xmlui/handle/123456789/762

x. Manahan, S. (2017). *Environmental chemistry* (10th ed.). CRC Press. https://doi.org/10.1201/9781315160474/ENVIRONMENTAL-CHEMISTRY-STANLEY-MANAHAN

xi. Manisalidis, I., Stavropoulou, E., Stavropoulos, A., & Bezirtzoglou, E. (2020). Environmental and health impacts of air pollution: A review. *Frontiers in Public Health, 8*. https://doi.org/10.3389/fpubh.2020.00014

xii. Ndetei, C. J. (2010). Noise Assessment and H2S Dispersion at Olkaria Geothermal Power Plant, Kenya (Issue 23). Retrieved from: https://orkustofnun.is/gogn/unu-gtp-report/UNU-GTP-2010-23.pdf

xiii. NEMA. (2014). Legal Notice No.34 E Environmental Management and Co-ordination Act (No 8 of 1999) the Environmental Management and Co-ordination (Air Quality) Regulations, 2014. Retrieved from: https://www.nema.go.ke/images/Docs/Regulations/air%20quality%20regulations2014-1.pdf

xiv. Nyairo, B., & Onyancha, D. (2018). Modeling H2S Dispersion from Proposed Menengai Geothermal Powerplant. *Shodhshauryam, International Scientific Refereed Research Journal*, 1(4), 2581–6306. www.shodhshauryam.com

xv. Rahman, F. A., Aziz, M. M. A., Saidur, R., & Bakar, W. A. W. A. (2018). A review of methods for measuring gas emission for combustion analysis in the industrial sector. *AIP Conference Proceedings, 2030*(1), 020291-1-020291–020298. https://doi.org/10.1063/1.5066932

xvi. Schnelle, J. K. B., & Brown, C. A. (2001). *Air Pollution Control Technology Handbook* (1st ed.). CRC Press. https://doi.org/10.1201/9781420036435

xvii. Sen, R., Mandal, A. K., Goswami, S., & Chakraborty, B. (2023). Prediction of Particulate Matter (PM2.5) Across India Using Machine Learning Methods. *Proceedings of the International Conference on Data Science and Applications, 553*, 545–556. https://doi.org/10.1007/978-981-19-6634-7_38

xviii. Turner, D. B. (1994). *Workbook of atmospheric dispersion estimates: An introduction to dispersion modeling* (2nd ed.). Lewis Publishers.

xix. Westbrook, J. (1999). Air Dispersion Models: Tools to Assess Impacts from Pollution Sources. *Natural Resources & Environment, 13*(4), 546–551. https://www.jstor.org/stable/40923918

xx. World Health Organization. (2019). Air pollution. Retrieved from https://www.who.int/health-topics/air-pollution#tab=tab_1

xxi. World Health Organization. (2021). WHO global air quality guidelines: Particulate matter (PM2.5 and PM10), ozone, nitrogen dioxide, sulfur dioxide, and carbon monoxide. Retrieved from: https://apps.who.int/iris/handle/10665/345329